
Amorphous and Crystalline Solids as Artifacts in SEM Images

Kitty L. Milliken

*Bureau of Economic Geology, University of Texas at Austin, Austin, Texas, U.S.A.
(e-mail: kitty.milliken@beg.utexas.edu)*

Terri Olson

Digital Rock Petrophysics, Golden, Colorado, U.S.A. (e-mail: tmolson8550@gmail.com)

ABSTRACT

Minerals can precipitate in samples after coring and after preparation for scanning electron microscope (SEM) imaging. Re-deposition of solids from ion milling also produces artifacts that can be observed in images. Both mineral precipitates and re-deposited solid mixtures can be obvious artifacts, but they can also be subtle and challenging to interpret as features that are not present in the subsurface. The most common mineral precipitates are hydrous calcium sulfate (gypsum or bassanite) and halite. Iron sulfate minerals are also commonly observed. These types of artifacts are illustrated, with examples from ion-milled, mechanically polished, and freshly broken surfaces of various sedimentary rocks. Recognition of these artifacts is important because they can reduce porosity and pore size in SEM images and can affect measurements of rock composition and interpretations of pore fluid chemistry.

INTRODUCTION

Various types of artifacts result from sample preparation and the process of creating images. These include topographic artifacts such as curtains, ion-beam striations, and shrinkage cracks as well as effects related to conductive coatings such as uneven charging and edge effects (Goldstein et al., 2003; Lemmens et al., 2011; Loucks et al., 2012). Another type of artifact, less widely recognized, is created by the precipitation of minerals and other solids after a core is acquired from the subsurface, and, in some cases, during or after polishing, milling, and coating of the specimen prior to

scanning electron microscope (SEM) imaging. Milling creates a very smooth surface (Ishitani and Yaguchi, 1996) with particular advantages for imaging of very small pores; the benefits and drawbacks of imaging mudrocks on fresh versus smooth surfaces are discussed by O'Brien et al. (2016).

Application of conductive coatings can be avoided if SEM imaging is performed at very low accelerating voltages; however, coatings allow easier access to high resolution observation under standard imaging conditions. Crystals precipitated on milled or polished surfaces are clearly a postpreparation phenomenon and readily recognizable as artifacts. Recognition of

mineral precipitation artifacts is important because they create new crystals and pore-filling textures that are not present in the subsurface. Reactions leading to the formation of mineral artifacts also provide important clues to the presence of reactive mineral components and pore fluids.

RE-DEPOSITION DURING MILLING

Milling by accelerated ions creates flat surfaces by ablation of materials that rise above the plane of the ion trajectories. Ablated material is deposited primarily within a field leeward of the milled surface. Localized deposition of ablated material within the area of

the milled surface (re-deposition), however, can create pore-fillings that are readily visible in backscattered and/or secondary electron images (Figure 1). The causes of re-deposition localization are uncertain, but may relate to local topography and to charges that build up on the edges of certain pores.

Features useful for discrimination of re-deposited material from natural mineral precipitates include: (1) non-euhedral shapes at the pore scale; (2) an asymmetric spatial distribution that is oriented with respect to the path of the ion beam; (3) composition that reflects the dominant elements in the material, but in ratios not characteristic of likely mineral phases; (4) the presence of metallic elements (e.g., Cu, Cr, Fe) derived from ablation of instrument components

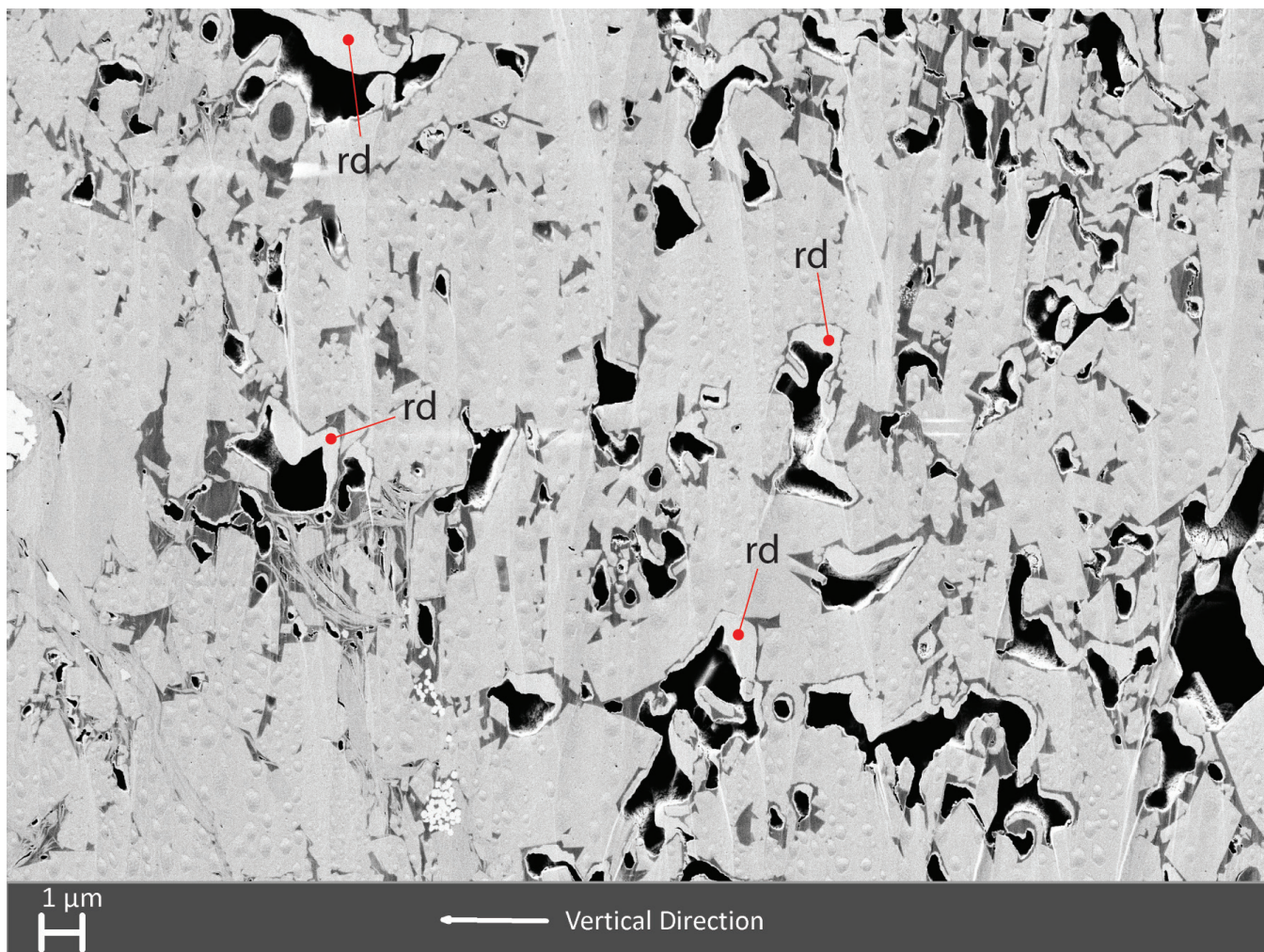


Figure 1. Combined secondary electron/backscattered electron image of ion-milled surface of a porous carl of the Niobrara Formation (Cretaceous). Material re-deposited during Ar-ion milling (rd, with red markers) has a substantially brighter backscattered electron coefficient than surrounding carbonate and other minerals, suggesting that it likely contains a component of metallic elements ablated from machine parts. The asymmetric spatial distribution, non-euhedral shapes, and the occurrence as a lining of organic pores further support the interpretation of this solid material as an artifact.

struck by the ion beam (Rob Reed, personal communication, 2015); and (5) accumulation of material upon organic surfaces that do not normally function as mineral nucleation sites.

Re-deposition is a serious issue in the case that it fills a significant volume of what would have been porosity, as it has in the specimen shown in Figure 1. Without the re-deposited material (around 5% of the image by area), the image displayed in Figure 1 would have about 13% porosity, around 60% more than the existing 8%.

MINERAL PRECIPITATION ON MECHANICALLY POLISHED AND MILLED SURFACES

Hydrous Ca-sulfate (gypsum, bassanite, and intermediate phases) and NaCl (halite) are the most commonly observed mineral precipitates on milled surfaces (Figures 2, 3, 4). Other minerals typical of

weathering-related rock alteration are also possible (Figures 3, 5). Precipitates on milled and polished surfaces typically display prominent localization, nucleating along cracks (Figures 2, 3) or in the vicinity of sulfide crystals (Figure 4) or organic matter (Figure 5). Halite precipitation suggests the presence of saline pore fluids that evaporate at some point after milling and before SEM observation. Hydrated Ca-sulfate precipitates most likely relate to the alteration of reactive sulfide minerals exposed to humid air in a reaction similar to that documented for weathering alteration of sulfide-rich mine tailings (e.g., Blowes et al., 1991).

POSTCORING MINERALS SEEN ON BROKEN SURFACES AND IN THIN SECTION

It is often less obvious that pore-filling crystal growth is recent (postcoring) and not part of the rock composition or texture in the subsurface. The similarity

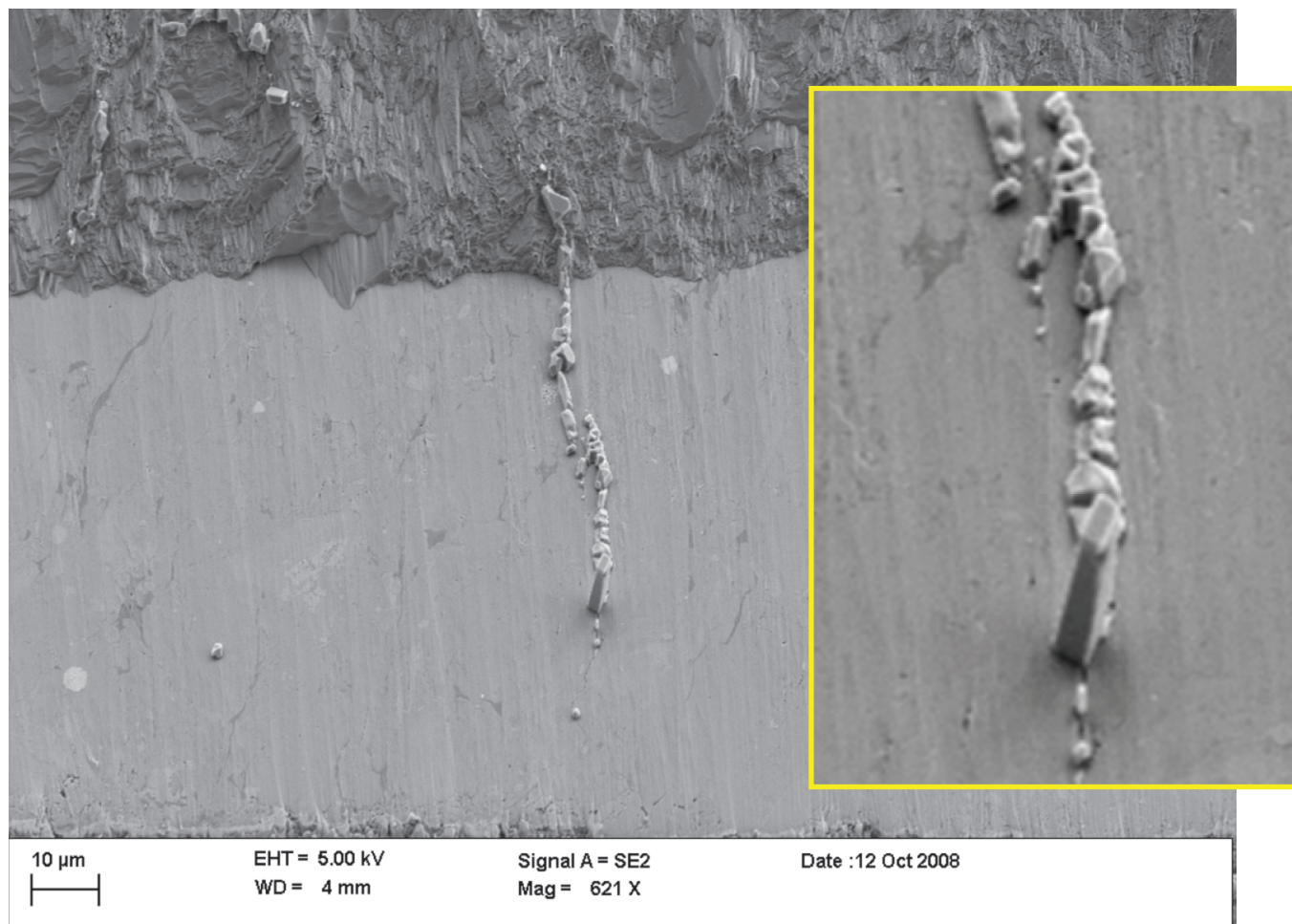


Figure 2. Secondary electron image. Gypsum crystal growth on an ion-milled surface of Woodford Shale (Devonian). Inset image shows prominent tabular crystal. Photo by Rob Reed, courtesy of Texas Bureau of Economic Geology.

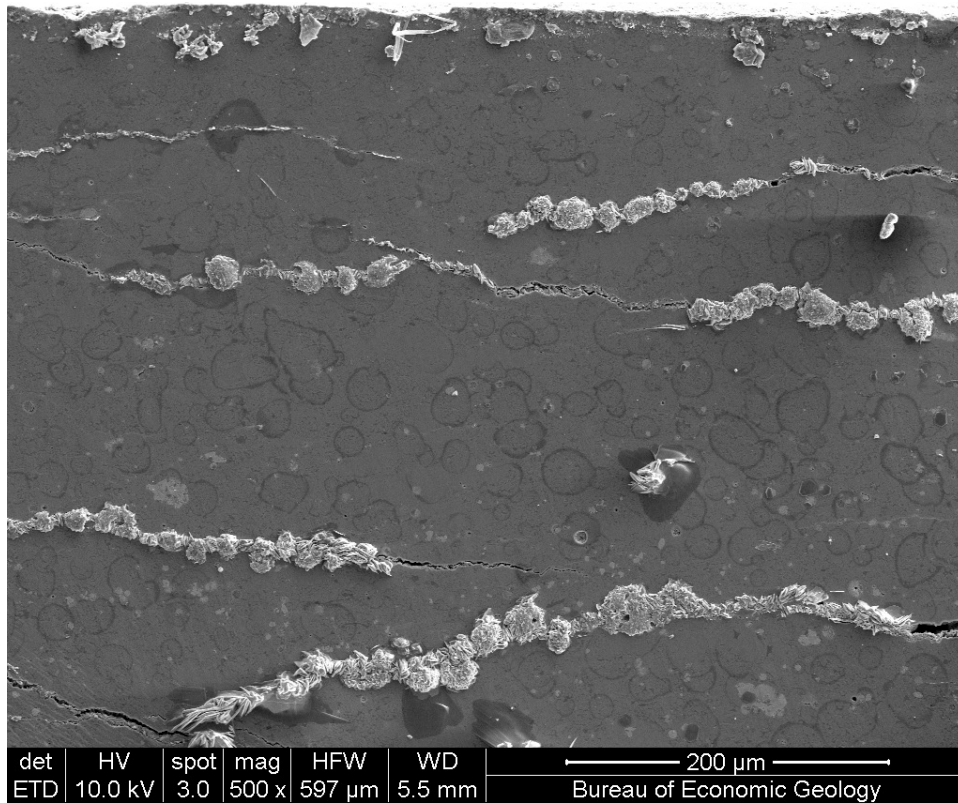


Figure 3. Secondary electron image. Fe-sulfate rosettes along cracks on a highly polished surface from the deep Wilcox Formation (Eocene, Gulf of Mexico). Photo by Rob Reed, courtesy of Texas Bureau of Economic Geology.

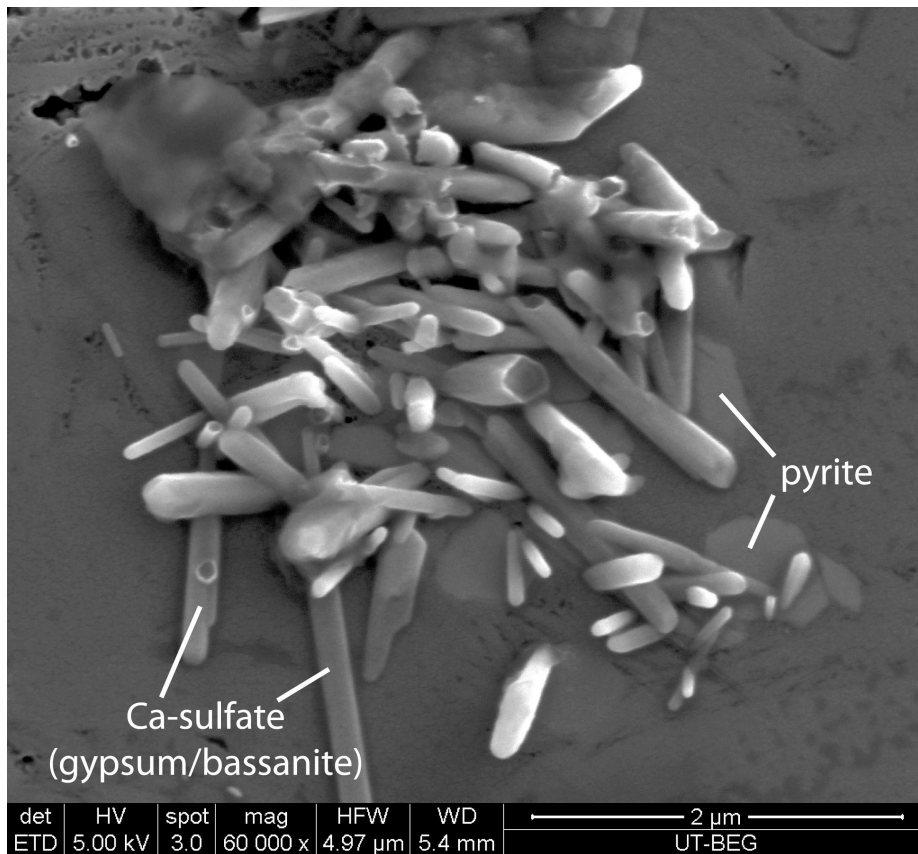


Figure 4. Secondary electron image of an Ar-ion milled surface. Calcium sulfate crystals localized on pyrite crystals in Marcellus Shale (Devonian). These crystals appeared within a few days of milling and coating of the specimen.

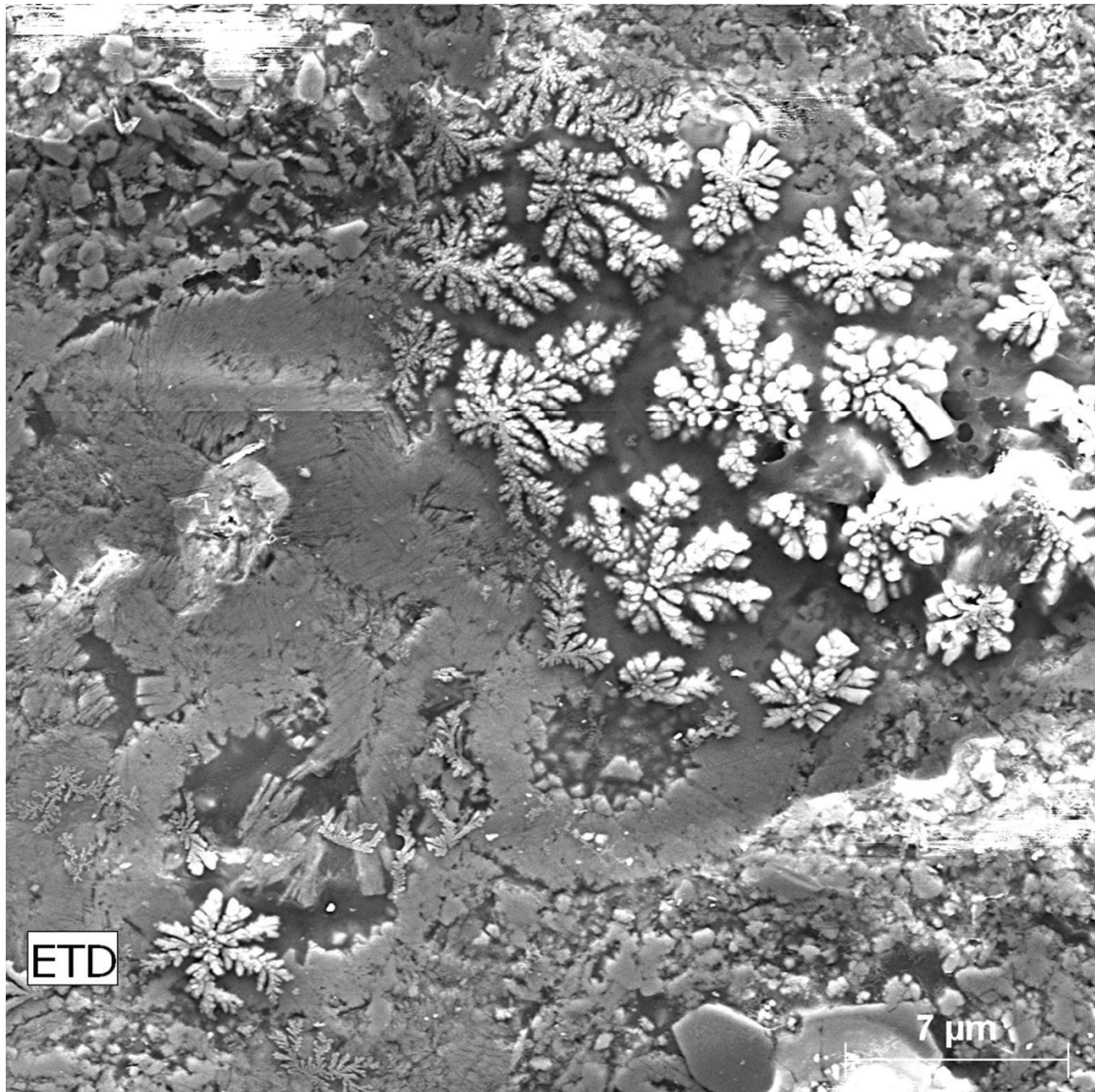


Figure 5. Secondary electron image of a polished, C-coated thin section. Brightly charging K, Na-bearing efflorescence is possible jarosite ($\text{KFe}_3(\text{OH})_6(\text{SO}_4)_3$) or a related mineral from the alunite group. Eagle Ford Formation (Cretaceous, South Texas). ETD = Everhart-Thornley detector. Photo by Suzan Ergene, Bureau of Economic Geology.

of certain pore-filling phases, both in composition (hydrous Ca-sulfates and halite) and crystal form, to those that are clearly artifacts on milled surfaces, brings us to the conclusion that certain pore fills are also artifacts (Figures 6, 7, 8).

These precipitates can be related in some cases to particular sample pressure-temperature histories (Simpson and Fishman, 2015) or to SEM preparation protocols such as solvent treatments. Compare the calcium sulfate (gypsum/bassanite) crystals in Figure 4 (polished surface) with those in Figure 6 (fresh broken surface).

Postcoring but presampling mineral precipitates within pores (Figures 7, 8) can be the most difficult to interpret. Recognition of fabric-integrated artifacts is important, however, because not only do these minerals fill pores and reduce apparent porosity and pore size, they also affect measurements of rock composition and interpretations of pore fluid chemistry (Blowes et al., 1991; Simpson and Fishman, 2015). Such artifacts may look natural in the sense of occurring within the rock fabric and may have a form similar to those of components that could exist in situ at reservoir conditions. Interpretation of such features as artifacts



Figure 6. Secondary electron image of apparent gypsum crystals that formed after extended soaking of the sample in toluene. Photo by Andrew Fogden, courtesy of Australian National University.

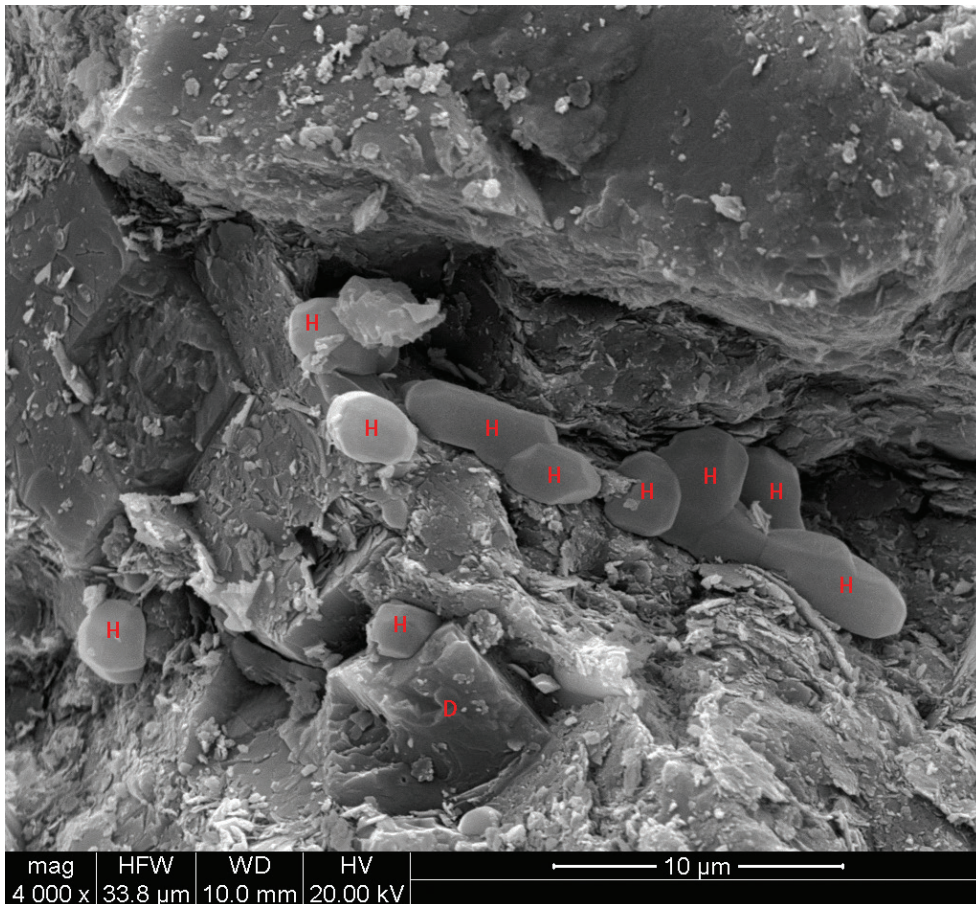


Figure 7. Secondary electron image showing halite (H) occluding pores and pore throats and partially coating dolomite (D), in the Three Forks Formation, (Devonian, Williston Basin, North America). The halite precipitated from pore fluids in the core, but after the core was subjected to ambient conditions at the surface. Photo courtesy of Hess Corporation.

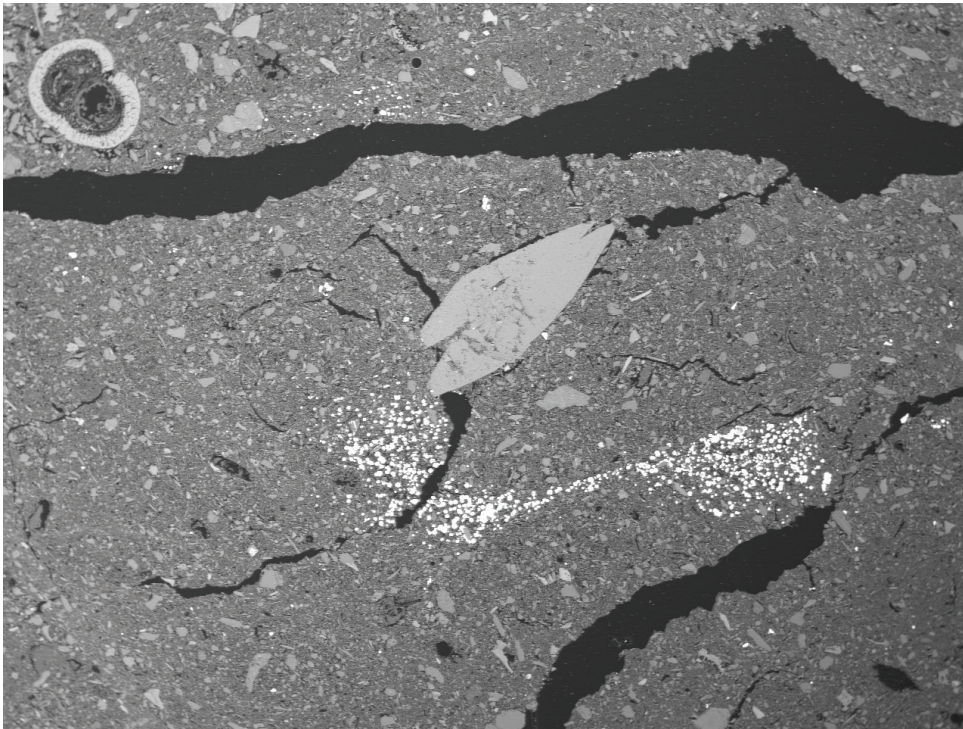


Figure 8. Backscattered electron image of postcoring bladed gypsum (large euhedral crystal) from IODP Site C0008 (Pleistocene, Nankai Margin). Such crystals were not observed in smear slides made shipboard shortly after coring (Milliken et al., 2012). SEM image of a polished surface at relatively low magnification (50 \times). Photo from Michael Strasser and Helen Eri Amsler, courtesy of ETH Zurich.

depends upon an understanding of the depositional conditions (e.g., thick clastics not related to evaporites) or on knowledge of the postcoring versus postsampling rock composition (e.g., Booth and Sefton, 1970; Schnitker et al., 1980; Milliken et al., 2012).

CONCLUSIONS

Crystalline or amorphous solids can form after coring and during preparation for SEM imaging.

Re-deposition of material ablated during ion milling can be recognized by spatial distributions and compositions that are unlike those of natural mineral components.

Postpreparation artifacts, especially ones formed after application of conductive coatings, are generally characterized by anomalous topography above the polished or milled surface and prominent charging.

Postcoring artifacts, formed before sampling and SEM preparation, are especially challenging to identify as they may be incorporated into the rock fabric (pore-filling). Identification of postcoring artifacts requires the petrographer to have a clear understanding of the mineral and fabric associations that are expected in the natural materials, and in some cases, to make an assessment of time-dependent changes in rock composition.

Halite related to evaporation of formation brines and sulfate minerals formed by rapid oxidation and

hydration reactions are the common mineral artifacts observed in both postcoring and postsampling preparation contexts.

Organic-rich mudrocks that contain briny fluids and sulfide minerals that are unstable under hydrous, oxygenated conditions are especially prone to develop mineral artifacts.

ACKNOWLEDGMENTS

This paper would not have been possible without the images contributed by our generous colleagues: Rob Reed (Texas Bureau of Economic Geology), Neil Fishman (Hess Corporation), Andrew Fogden (FEI Oil & Gas), Michi Strasser and Eri Amsler (ETH Zurich), and Suzan Ergene (Middle East Technical University). We also thank Mark Curtis, Eric Goergen, Rob Reed, and Patrick Smith for discussions during the early stages of manuscript preparation. This publication is authorized by the Director, Bureau of Economic Geology.

REFERENCES

- Blowes, D. W., E. J. Reardon, J. L. Jambor, and J. A. Cherry, 1991, The formation and potential importance of cemented layers in inactive sulfide mine tailings, *Geochimica et Cosmochimica Acta*, v. 55, p. 965–978.

- Booth, G. H., and G. V. Sefton, 1970, Vapour phase inhibition of Thiobacilli and Ferrobacilli: A potential preservative for pyritic museum specimens, *Nature*, v. 226, p. 185–186.
- Goldstein, J., E. D. Newbury, D. C. Joy, C. E. Lyman, P. Echlin, E. Lifshin, L. Sawyer, and J. R. Michael, 2003, *Scanning electron microscopy and x-ray microanalysis* (3rd ed.), New York, Springer-Verlag, 689 p.
- Ishitani, T. and Yaguchi, T., 1996, Cross-sectional sample preparation by focused ion beam: A review of ion-sample interaction: *Microscopy Research and Technique*, v. 35, p. 320–333.
- Lemmens, H., A. R. Butcher, and P. W. S. K. Botha, 2011, FIB/SEM and SEM/EDX: A new dawn for the SEM in the core lab? *Petrophysics*, v. 52, no. 6, p. 452–456.
- Loucks, R. G., R. M. Reed, S. C. Ruppel, and U. Hammes, 2012, Spectrum of pore types and networks in mudrocks and a descriptive classification for matrix-related mudrock pores, *AAPG Bulletin*, v. 96, no. 6, p. 1071–1098.
- Milliken, K. L., Comer, E. E., and Marsaglia, K. M., 2012, Data report: Modal sand composition at Sites C0004, C0006, C0007, and C0008, IODP Expedition 316, Nankai accretionary prism, *in* Kinoshita, M., Tobin, H., Ashi, J., Kimura, G., Lallemand, S., Scretton, E. J., Curewitz, D., Masago, H., Moe, K. T., and the Expedition 314/315/316 Scientists, *Proc. IODP*, 314/315/316: Washington, DC (Integrated Ocean Drilling Program Management International, Inc.), DOI:10.2204/iodp.proc.314315316.221.2012.
- O'Brien, N. R., C. A. McRobbie, R. M. Slatt, and E. T. Baruch-Jurado, 2016, Unconventional gas–oil shale microfabric features relating to porosity, storage, and migration of hydrocarbons, *in* T. Olson, ed., *Imaging unconventional reservoir pore systems: AAPG Memoir 112*, p. 43–64.
- Schnitker, D., L. M. Mayer, and S. Norton, 1980, Loss of calcareous microfossils from sediments through gypsum formation, *Marine Geology*, v. 36, p. M35–M44.
- Simpson, G. A., and N. S. Fishman, 2015, Using advanced logging measurements to develop a robust petrophysical model for the Bakken Petroleum System, *Petrophysics*, v. 56, no. 5, p. 457–478.